Indoor Object Positioning using Smartphone and RFID or QRCode

Riccardo Carotenuto
Department of Information Engineering, Infrastructures and Sustainable Energy (DIIES) University Mediterranea of Reggio Calabria
Reggio Calabria, Italy
r.carotenuto@unirc.it

Massimo Merenda
Department of Information Engineering, Infrastructures and Sustainable Energy (DIIES) and HWA s.r.l.-Spin Off of the University Mediterranea of Reggio Calabria
Reggio Calabria, Italy
massimo.merenda@unirc.it

Demetrio Iero
Department of Information Engineering, Infrastructures and Sustainable Energy (DIIES) and HWA s.r.l.-Spin Off of the University Mediterranea of Reggio Calabria
Reggio Calabria, Italy
demetrio.iero@unirc.it

Francesco Giuseppe Della Corte
Department of Information Engineering, Infrastructures and Sustainable Energy (DIIES) and HWA s.r.l.-Spin Off of the University Mediterranea of Reggio Calabria
Reggio Calabria, Italy
francesco.dellacorte@unirc.it

***Abstract*—Positioning objects such as appliances inside rooms has become of fundamental importance in the Internet o Things (IoT) and òòin-home automation, as well as in augmented reality (AR). A new positioning system based on a smartphone and radio-frequency identification (RFID) tags applied to the objects to be localized is presented. The 3D positioning of the smartphone is obtained through an ultrasound system while its orientation in space is obtained with the onboard magnetometers and accelerometers. When a certain RFID tag is read through the near-field communication (NFC) interface of the smartphone, from its distance and from the orientation of the smartphone that reads it, the 3D position of the tagged object is obtained. The system architecture is explained and simulation results are presented. Positioning accuracy of about ten centimeters is achieved**

Keywords—Indoor positioning, Ultrasonic positioning, RFID tag

I. INTRODUCTION

Tridimensional positioning with high spatial resolution is able to open new applications in the fields of IoT and domotics, as well as logistics and mobile asset management. [1-8]. Positioning of objects, like home or office assets, is crucial for spatial-based control of operation. Many attempts to develop indoor positioning systems with sufficient resolution and reasonable cost have been reported in the literature [9], however still open questions are sufficient accuracy, low cost, miniaturizable, and operation relying on small batteries. Main technologies used in the proposed systems include Radio Frequency (RF) signals [10], video cameras, laser beams [11], infrared sensors [12], magnetic sensors [13], and ultrasonic waves [14]. Ultrasonic wave-based systems provide spatial distances and positions with a high degree of accuracy at a relatively low cost. [15].

Ultrasonic techniques compute positioning from ranging measurements from a set of reference points. The most used techniques are time of arrival (TOA) and time difference of arrival (TDOA). The methods that are based on the TOA require the exact knowledge of when (time of emission, TOE) the emitter starts to emit the ultrasonic signal, thus requiring a tight synchronization between emitter and receiver, usually obtained using a suitable RF communication channel [16-17]. Unfortunately, a sufficiently tight synchronization cannot be achieved using a smartphone due to its multiple firmware and software layers, which are loosely synchronized each other.

When the required tight synchronization between emitter and receiver is not available, it is possible to obtain a positioning through pseudo range multilateration by only measuring TOAs. This technique is based on the differences in the TOAs of two or more received signals, using one of them as a reference, thus obtaining TDOAs. Subsequently, TDOAs are converted in distance differences. The minimur requirement is of at least three distance differences from four reference points to obtain the tridimensional MD positioning as an intersection of three hyperboloids. In [18-19], solutions based on both TDOA and arrival frequency difference (FDOA) were presented to include target speed data. The solution provided in [20] uses smartphones acting as acoustical receivers for an experimental 2D positioning for indoor navigation. An iterative least square matrix method provides TDOA positioning. The accuracy of the sub-decimeter positioning has been reported as well as an analysis of the acoustic reception quality relative to the angle of rotation of the smartphone with the emitters. A simultaneous 2D TDOA positioning of several transmitters and a moving receiver is presented in [21]. The positioning is obtained by iteratively solving a non-linear optimization problem of TDOA using a physical mass-spring representation of the error function. However, this solution requires a significant computational cost that translate into in a powerful processor and a big battery. In [22], three-dimensional positioning is obtained using five reference points (beacons) and four TDOAs. This redundancy allows the linearization and thus algebraic solution. The simulated results were also reported therein. In [23], is showed a room-level positioning system for the navigation of robots, with experimental results in the 2D plane.

Another indoor ultrasonic positioning system uses a form of TOF positioning without using any sort of reference signals to indicate the ultrasonic TOE [24]. It uses a combination of angle of arrival (AOA) and TOF with an intelligent timing recovery algorithm that can indirectly estimate the proper timing at runtime. However, this method presents some critical problems, such as clock drift, the need for three

XXX-X-XXXX-XXXX-X/XX/$XX.00 ©20XX IEEE

DOI: 10.23919/SpliTech49282.2020.9243703

microphones, and the fact that the necessary iterative calculation is not easily obtainable with a low power design.

A system was proposed that, inspired by that described above [24], overcomes some of its critical elements [25]. The synchronism is indirectly estimated from the time difference of arrival (TDOA) of the ultrasonic signals. The system uses four ultrasonic beacons, while the MD has a single ultrasonic receiver. All the calculation are performed on each MD and the calculated position is private (infrastructure is not aware of the number or identity of the MDs). Simulations and experimental results have been provided. A moving MD estimates TO using only TDOA information using a mathematically closed form derived from the intersection of hyperboloids, which is however very sensitive to uncertainty. [26-27]. MD estimates TO without prior information. Because of the clock drift, the MD does not see a constant TO but a time ramp with a slope proportional to the drift. An estimate of true TO is obtained by using a ramp follower that converges even in the presence of clock drift. In a second phase, it is possible to get a more accurate estimate of the MD position through the intersection of spheres with radii obtained through estimates of converging TO and measured TOAs. All computations are performed using closed form formulas, minimizing computational load, complexity, size, and energy consumption of the MD.

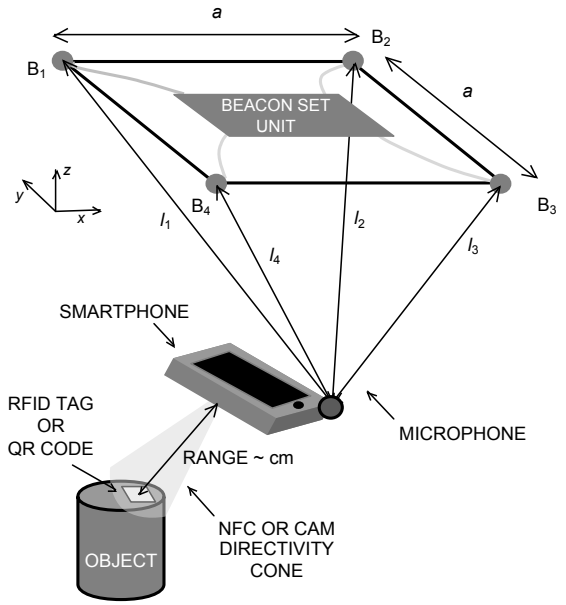

Fig. 1. System architecture. The Beacon Set Unit emits the ultrasonic chirp signals through the four beacons B_1, B_2, B_3, and B_4 placed at the corners of a square; the smartphone, which is running a specific application, receives through its microphone four ultrasonic signals and calculates its own position. The position of the tag is found by adding information of space orientation and range,. The beacons belong to the same circuit and are intrinsically synchronized with each other.

In this work, as original contribution, a second step is added. Once the smartphone positioning is obtained, it is possible to compute the position of the asset to be located. This is obtained in a two steps process, here only depicted and beyond the scope of this work. First, a RFID tag is placed on the asset containing all the required information on the asset itself, for example spatial occupancy, power supply required, minimal distance from other particular assets, etc. The application running on the smartphone, which is in the neighborhood of the asset, reads through its NFC interface the asset information. Secondly, the same application associates the asset to the smartphone position plus a spatial translation. The translation and its direction is estimated from smartphone orientation (azimuth and zenith angles from onboard compass and accelerometers) and range (from RSSI data), i.e. via a coordinate transformation, taking into account the NFC antenna directivity.

This system can be used in an indoor environment by a number of different devices that meet a set standard, similar to how the GPS system is used. In the long run, devices such as smartphones, tablets, and laptops could take advantage of a standard indoor positioning infrastructure to easily obtain indoor positioning and navigation in places such as shopping malls, hospitals, and stations.

The document is structured as follows: section 2 explains how the proposed system works, while section 3 reports the results of the simulations. Finally, section 4 reports the conclusions of the paper.

II. System architecture and operation

An innovative system for object positioning in indoor environment using a to the smartphone with NFC interface or QR code, is presented.

Positioning is achieved in two steps (see Figure 1): 1) the smartphone is positioned absolutely within a specific reference system using an ultrasonic system [25]. At the same time, the smartphone orientation in the space is computed using onboard accelerometers and magnetometers, just as it is usually done by smartphone AR applications; 2) The smartphone NFC reads the RFID tag [28] placed on the object to be located, and from the RSSI and known antenna directivity information it is able to determine approximated distance and orientation from the smartphone. The final object positioning is obtained by geometrical composition of the data computed.

The ultrasonic system consists of four coplanar emitters, placed at the corners of a square of side a, designed to be positioned on the ceiling of a room. At first, only a smartphone is considered, however the following considerations can be extended to any number of smartphones.

The four beacons emit ultrasonic signals in a predefined sequence (i.e., 1, 2, 3, 4, $T_{SILENCE}$, 1, 2, 3, 4...) starting from the time $t_{0BEACONS}$, and the time interval between emissions is $T_{REPETITION}$ (see Fig. 2). Each emission duration is $T_{EMISSION} < T_{REPETITION}$. The beacons belong to the same circuit and are intrinsically synchronized with each other. The sequence of the four signals is repeated in identical frames emitted at regular time intervals of duration T_{FRAME} (frame repetition time). The ultrasonic signal is a chirp that allows to take full advantage of correlation during ranging.

The smartphone records the ultrasonic signal coming from the Beacon Set for a duration time of T_{FRAME}, according to its internal timing.

Therefore, two distinct periodic processes can be considered: 1) The ultrasonic emission, at beacon set, frame repetition which starts at $t_{0BEACONS}$; 2) the listening at the smartphone whose window starts at t_{0SP} (where SP stands for SmartPhone, see Figure 2). They are repeated with equal periods but with different starting times. There is, therefore, a lag or time offset between the two processes $T_{OFFSET} = t_{0BEACONS} - t_{0SP}$ that is unknown.

Typically, one of the synchronization techniques known in the literature is used to estimate T_{OFFSET}, for example Reference Broadcasting [29-31], which however require additional hardware (wires, RF, etc.) and protocols.

On the contrary, here we used a solution that avoids synchronization hardware allowing the recovery of T_{OFFSET} is proposed. The smartphone application cross-correlates the received chirp signal and a copy of the chirp stored in advance in the smartphone, after proper properly sampling and conversion from analog to digital. The position of the cross-correlation maximum indicates the point in time where the received signal and the stored chirp are best aligned. The lag τ, or inter-signals displacement, corresponding to the cross-correlation peak is proportional to the TOA referred to the local clock.

Since the smartphone does not know the time of emission of each ultrasonic signal, it is not able to estimate the TOF, but only the TOAs of each signal referred to the local clock, which are TOA_1, TOA_2, TOA_3, TOA_4, respectively. From these, three TDOA dt_j (j = 1, 2, 3) are obtained:

$$\begin{aligned} dt_1 &= TOA_2 - TOA_1 \\ dt_2 &= TOA_3 - TOA_1 \\ dt_3 &= TOA_4 - TOA_1. \end{aligned} \tag{1}$$

Knowing the propagation velocity of the sound wave in the air c_{air}:

$$c_{air} = 331.5\sqrt{1+\frac{T}{273.15}}, \tag{2}$$

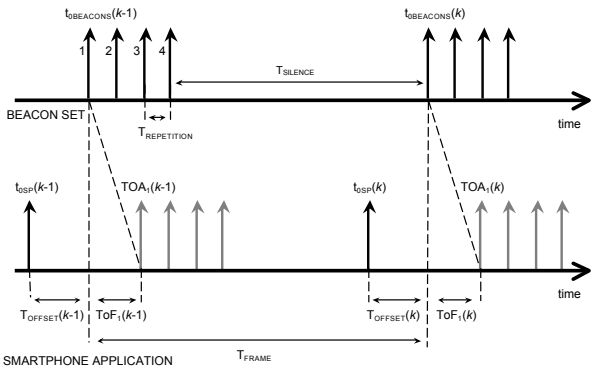

Fig. 2. Time diagram for the Beacon Set and the smartphone running application (not in scale): the four beacons emit ultrasonic signals in a predefined sequence (i.e., 1, 2, 3, 4, $T_{SILENCE}$, 1, 2, 3, 4...) starting from the time $t_{0BEACONS}$, and the time interval between emissions is $T_{REPETITION}$.

the range differences d_j (j = 1, 2, 3) from the time differences are calculated as:

$$\begin{aligned} d_1 &= dt_1 \cdot c_{air} = l_2 - l_1 \\ d_2 &= dt_2 \cdot c_{air} = l_3 - l_1 \\ d_3 &= dt_3 \cdot c_{air} = l_4 - l_1, \end{aligned} \tag{3}$$

where l_1, l_2,…l_4 are the distances between the smartphone and the four beacons. Here, it is assumed that in a room the air flows and temperature gradient are well-controlled control, as usual. Small fluctuations slightly affect positioning accuracy. Otherwise, methods based on direct or indirect measurement of the speed of sound along the propagation path [32] can be adopted. When required, in environments with fast temperature variations, a direct temperature reading can be carried out by the smartphone onboard temperature sensor. From (4), by solving the intersection of hyperboloids, the coordinates (x, y, z) of the smartphone are finally calculated:

$$\begin{cases} d_1 = l_2 - l_1 = \sqrt{(x-x_{RP2})^2 + (y-y_{RP2})^2 + (z-z_{RP2})^2} - l_1 \\ d_2 = l_3 - l_1 = \sqrt{(x-x_{RP3})^2 + (y-y_{RP3})^2 + (z-z_{RP3})^2} - l_1 \\ d_3 = l_4 - l_1 = \sqrt{(x-x_{RP4})^2 + (y-y_{RP4})^2 + (z-z_{RP4})^2} - l_1, \end{cases} \tag{4}$$

where $X_{RPi} = (x_{RPi}, y_{RPi}, z_{RPi})$ is the reference position of the ith (i = 1, 2,…4) beacon.

The relative position of the smartphone with respect to the emitters, the distance between the emitters and the noise level greatly influence the accuracy of the solution. In particular, whenever the smartphone is located in points of space equidistant at least by two emitters, or in their proximity, the solutions of (4) are affected by errors whose entity can be significant. Considering the arrangement of the four beacons at the corners of a square of side a, with coordinates $X_{RP1} = (0, 0, 0)$, $X_{RP2} = (a, 0, 0)$, $X_{RP3} = (a, a, 0)$, $X_{RP4} = (0, a, 0)$, respectively, the (4) can be rewritten as follows:

$$\begin{aligned} d_1 &= \sqrt{(x-a)^2 + y^2 + z^2} - l_1 \\ d_2 &= \sqrt{(x-a)^2 + (y-a)^2 + z^2} - l_1 \\ d_3 &= \sqrt{x^2 + (y-a)^2 + z^2} - l_1, \end{aligned} \tag{5}$$

and rearranging the terms and rewriting the first and third equations, is obtained:

$$\begin{aligned} (x-a)^2 + z^2 &= (d_1 + l_1)^2 - y^2 \\ (y-b)^2 &= (d_3 + l_1)^2 - x^2 - z^2, \end{aligned} \tag{6}$$

By replacing the (6) in the second of the (5), is obtained:

$$\begin{aligned} &(d_2 + l_1)^2 = (d_1 + l_1)^2 - y^2 + (d_3 + l_1)^2 - x^2 - z^2 = \\ &= (d_1 + l_1)^2 + (d_3 + l_1)^2 - l_1^2. \end{aligned} \tag{7}$$

Resolving the (7) for l_1, finally is obtained:

$$l_1 = \frac{d_2^2 - d_1^2 - d_3^2}{2(d_1 + d_3 - d_2)}. \tag{8}$$

Equation (8) gives an estimate of l_1 and from this, through the (3), of l_2, l_3, and l_4. From l_1, $TOF_1 = l_1/c_{air}$ is obtained, and from this, knowing $TOA_1 = TOF_1 + T_{OFFSET}$, then T_{OFFSET} is finally estimated:

$$T_{OFFSET} = TOA_1 - TOF_1. \tag{9}$$

As thoroughly discussed in [25], the accuracy of the current estimate of T_{OFFSET} from (9) strongly depends on the position of the smartphone with respect to the four beacons. The (8) produces large error in some positions, where the denominator becomes very small or almost zero. In the space points set where $d_1 + d_3 - d_2 = 0$ there is an unlimited error and (8) can be considered as "blind". Each T_{OFFSET} estimated

directly from (8) is therefore affected by a considerable noise (see Fig. 6).

It is worth noting that T_{OFFSET} is the same for all the beacons belonging to the same synchronous circuit, and, above all, T_{OFFSET} is the same for any position of the smartphone.

The obtained noisy value of T_{OFFSET} can be used to refine the estimate of the true value of T_{OFFSET} at each positioning operation. If T_{OFFSET} were really constant, in order to obtain an accurate estimate of the T_{OFFSET}, it would be enough to make an average of the noisy values of the rough T_{OFFSET} estimates coming from (8), provided that the noise has zero mean value. This approach was followed by [24], which used a moving average.

However, in presence of intrinsic drift between the two clocks, the above approach is unsuitable. In fact, even if nominally the clocks of the beacon set and of the smartphone have the same frequency, in practice the frequencies of the two clocks differ for some part per million (ppm) and there is a not negligible clock drift over time. Considering a commercial quartz clock, a typical value for clock total uncertainty is 100 ppm, depending on the temperature, manufacture, and aging of the clock components. Clock drift, which is one of the components of the total uncertainty of a clock, produces remarkable effects. If for example the clock frequency of our beacon set and smartphone systems is 20 MHz, and they differ by 50 ppm, after one second, in the worst case, the two clocks differ by 1000 clock periods or 100 μs. This difference produces a measurement error of about 3.4 cm assuming a sound speed of 343 m/s. Over the course of time an error of 3.4 cm is accumulated for every additional second of the system operation, and therefore after 60 s the error exceeds 2 m, even starting from the unrealistically favorable hypothesis of initial synchronization between the two clocks

Based on the considerations made, it is possible to estimate T_{OFFSET} as a ramp over time, then $T_{OFFSET}(k)$ is estimated as a function of time, where k is a time index. In particular, due to the presence of a high noise level on the single T_{OFFSET} estimates from (9), it is appropriate to estimate the clock drift value through a sort of time filter, for example a ramp follower [33]. We also hypothesized that the value of the drift, or the slope of the time ramp, remains reasonably constant or very slow varying during the time interval of the operations of the system:

$$
\begin{aligned}
&e(k) = y(k) - ref(k)\\
&\begin{bmatrix} x_1(k+1) \\ x_2(k+1) \end{bmatrix} = \begin{bmatrix} 1 & 0 \\ 0.01 & 1 \end{bmatrix} \begin{bmatrix} x_1(k) \\ x_2(k) \end{bmatrix} + \begin{bmatrix} 0.01 \\ 5\cdot 10^{-5} \end{bmatrix} e(k)\\
&y(k+1) = K \begin{bmatrix} 1 & 1 \end{bmatrix} \begin{bmatrix} x_1(k+1) \\ x_2(k+1) \end{bmatrix},
\end{aligned}
\tag{10}
$$

where k is the kth time step of T_{FRAME} duration, i.e., the repetition time of the positioning operation, $ref(k)$ is the noisy ramp to be followed, i.e., the current value of $T_{OFFSET}(k)$, $y(k) = T^*_{OFFSET}(k)$ is the estimate of the true $T_{OFFSET}(k)$ after the noise rejection, $x_1(k)$ and $x_2(k)$ are the internal states of the ramp follower, and K is a constant parameter tuned by trial and error procedure. The smaller is K value, the greater the noise rejection and convergence time of the ramp follower.

The $T^*_{OFFSET}(k)$ estimate allows finding the estimates $l^*_i(k)$ through the following:

$$
\begin{aligned}
l^*_1(k) &= [TOA_1(k) + T^*_{OFFSET}(k)]\cdot c_{air}\\
l^*_2(k) &= [TOA_2(k) + T^*_{OFFSET}(k)]\cdot c_{air}\\
l^*_3(k) &= [TOA_3(k) + T^*_{OFFSET}(k)]\cdot c_{air}\\
l^*_4(k) &= [TOA_4(k) + T^*_{OFFSET}(k)]\cdot c_{air}.
\end{aligned}
\tag{11}
$$

The $T^*_{OFFSET}(k)$ sequence thus obtained, although heavily filtered over time, allows to obtain the $TOF(k)_i = TOA(k)_i + T^*_{OFFSET}(k)$ sequence and therefore to use the intersection of spheres:

$$
\begin{cases}
l_1^{*2} = x^2 + y^2 + z^2\\
l_2^{*2} = (x-a)^2 + y^2 + z^2\\
l_3^{*2} = (x-a)^2 + (y-a)^2 + z^2\\
l_4^{*2} = x^2 + (y-a)^2 + z^2,
\end{cases}
\tag{12}
$$

which produces much more accurate results than the intersection of hyperboloids (4), therefore overcoming the issue of noisy results from (4). Ultimately, this approach allows trajectories to be tracked with reduced noise even in the presence of abrupt variations.

Equation (12) allows calculating the estimate of the position of the smartphone at the kth positioning frame through the simplified spherical equations intersection solution [25]. By picking in all combinations three sphere equations at a time from the available four (12), four sets of coordinates for the position of the smartphone are obtained. The results are averaged, making it more robust against small and unbiased errors on the estimates of the four distances:

$$
\begin{cases}
x = \dfrac{1}{4}\sum_{h=1}^{4} x_h\\
y = \dfrac{1}{4}\sum_{h=1}^{4} y_h\\
z = \dfrac{1}{4}\sum_{h=1}^{4} z_h.
\end{cases}
\tag{13}
$$

Once the smartphone is absolutely 3D-located inside the indoor space, its orientation is calculated using the onboard accelerometers and compass, as usually done in AR applications.

Subsequently, using the integrated NFC interface, the smartphone is able to find the RFID tag applied on the target to be localized, which is assumed to be a few centimeters from the smartphone. The spatial orientation information of the smartphone allows to better specifying the positioning of the object, in relation to the RSSI in conjunction with the known directivity of the onboard NFC reader. At this point it is possible to store or transmit to an external database, linked to home automation or IoT management applications, the pairing between the object identifier and its absolute three-dimensional position in the reference system given by the beacon set. A block diagram of the proposed positioning algorithm, as executed by suitable application running on the smartphone is shown in Figure 3.

III. Algorithm Simulation Setup and Results

The beacon system is fixed at the center of the ceiling of a 4×4×3 m^3 room. The beacons are fixed at the corners of a square having side a = 50 cm, so as to constitute an element that can easily be integrated into a typical room ceiling panel. The simulation computations start from the knowledge of the four TOAs, which are detected in the correlation between received signal and signal stored in memory with uncertainty ΔTOA [17][30]. In the following simulations, $F_S = 1/T_S$ = 96 kS/s and ΔTOA = ±T_S/2 have been set. Assuming the sound speed 343 m/s, the time interval of T_S corresponds to a space interval of 3.6 mm. A random value for the starting $T_{OFFSET}(0)$ and a Beacon Set-smartphone relative clock drift of 100 ppm has been assumed. In the presence of clock drift, we have:

$$T_{OFFSET}(k) = T_{OFFSET}(0) + \Delta_{CLOCK} \cdot k, \qquad (15)$$

where Δ_{CLOCK} = 12.5 μs is computed taking into account that a 200 ppm clock drift applies to an external 32768 Hz crystal, from which the microprocessor clock is derived, and T_{FRAME} is 0.1 s.

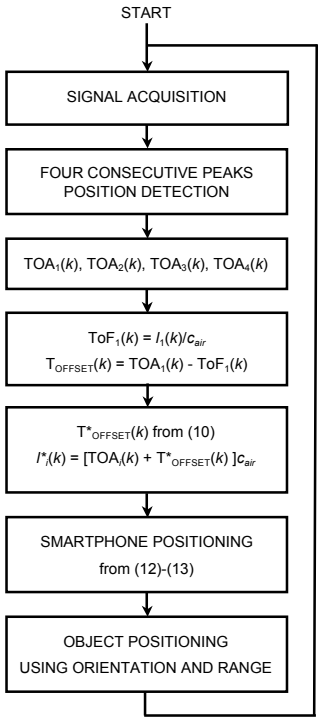

Fig. 3. Block diagram of the proposed positioning algorithm that operates in an infinite loop after initializing $T_{OFFSET}(0) = 0$ and $T^*_{OFFSET}(0) = 0$.

In the simulation, the smartphone moves along a preset 3D elliptical trajectory (see Figure 4) and the T_{FRAME} is 0.1 s (i.e., frame rate 10 Hz). The rectangular trajectory is repeated for a total of 1000 positioning frames to show the convergent behavior of the T_{OFFSET} recovery process. Figure 4 shows the estimated trajectory compared to the true one, indicated by the last 500 position estimates, i.e., after the initial algorithm convergence. The overall 3D positioning error e_{ED} at each point is given by the Euclidean distance between each ground truth point and the estimated one. Figure 5 reports the e_{ED} behavior along the 1000 positioning frames. Figure 6 shows the cumulative distribution function (CDF) of the smartphone positioning over the last 500 positioning frames and of the last 100 trajectory points after convergence. The results obtained demonstrate that 3D positioning with acceptable error (less than 6 cm) can also be obtained with the limited sampling frequency (96 kS/s) provided by the typical smartphone hardware, differently from the relatively high sampling frequency (200 kS/s) considered in [25].

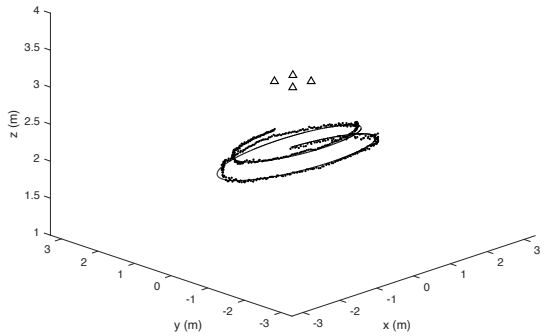

Fig. 4. Simulated trajectory of the moving smartphone (line) and estimated positioning (dots): Last 500 positioning frames. Beacons are indicated by triangles.

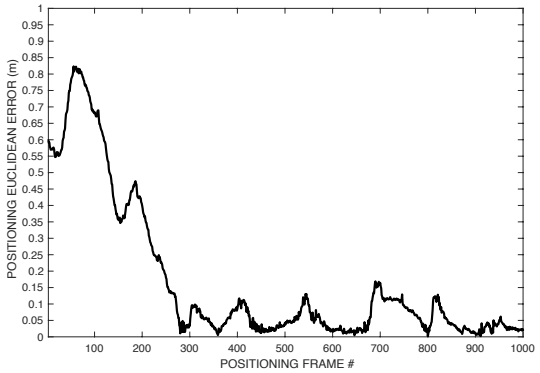

Fig. 5. Decreasing positioning error e_{ED} over 1000 successive positioning frames.

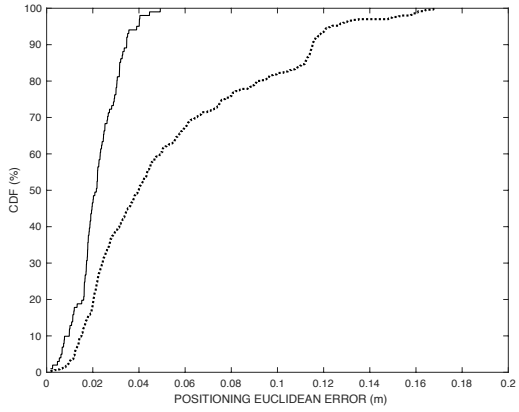

Fig. 6. Cumulative error distributions (percent of readings with error less than the value of a given abscissa) of the smartphone positioning over the last 500 positioning frames (dotted line) and of the last 100 trajectory points (solid line) after convergence transient.

Finally, it is reasonable to assume that the error introduced by the orientation measures (zenith and azimuth angles) and range (RSSI), plus the uncertainty due to the inaccurate information from RSSI and antenna directivity is

in any case of the same order of the distance between smartphone and tag or even less, that is, a few centimeters.

When the NFC interface is unavailable it is possible to use QR code instead. The built-in cam scans a QR code tag placed on the asset to be located, replacing the RFID tag. In this case the ranging information is obtained from lens focusing data. That, in conjunction with smartphone orientation, allows a positioning with similar accuracy.

IV. Conclusions

In this work, a new system for indoor object positioning using smartphone, ultrasonic signals, and NFC or QR code is presented. In a first step, the 3D positioning of the smartphone is obtained through an ultrasound system while its orientation in space is obtained with the onboard magnetometers and accelerometers. In a second step, the onboard NFC interface reads the RFID tag placed on the object to be positioned and the RSSI is recorded. The composition of the positioning information of the smartphone, the spatial orientation, the NFC reader diagram and the RSSI obtained, allows to define with a low approximation the three-dimensional position of the RFID tag and therefore of the object on which it is positioned. When the NFC interface is unavailable it is possible to use onboard cam and a QR code tag instead. The system architecture and operation were described and simulation results presented. Overall positioning accuracy of about ten centimeters was achieved, under reasonable assumptions. Many applications and services within the domotics and Internet of Things can benefit of the presented system.

References

[1] Zhang, D., Xia, F., Yang, Z., Yao, L., Zhao, W, In the Proceedings of Localization Technologies for Indoor Human Tracking. 2010 5th International Conference on Future Information Technology, Busan, South Korea, 21-23 May 2010; pp. 1-6.

[2] Przybyla, R. J., Tang, H. Y., Shelton, S. E., Horsley, D. A., 3D ultrasonic gesture recognition. Proceedings of 2014 IEEE Int. Solid-State Circuits Conference Digest of Technical Papers (ISSCC), San Francisco, CA, USA, 9-13 February 2014; pp. 210-211.

[3] Ionescu, R., Carotenuto, R., 3D Localization and Tracking of Objects Using Miniature Microphones. Wirel. Sens. Netw., 2011, 3, 147-157,.

[4] Carotenuto, R., Touchless 3D gestural interface using coded ultrasounds. Proceedings of 2012 IEEE International Ultrasonics Symposium, Dresden, Germany, 7-10 October 2012, pp.146-149.

[5] Ebisawa, Y., A pilot study on ultrasonic sensor-based measurement of head movement. IEEE Trans. Instrum. Meas., 2002, 51, 1109-1115.

[6] Kasprzak, H. T., "Ultrasonic measurement of fine head movements in a standard ophthalmic headrest," IEEE Trans. Instrum. Meas., 2010, 59, pp. 164-170.

[7] Torres-Solis, J., Falk, T. H., A review of indoor localization technologies : towards navigational assistance for topographical disorientation. Ambient Intell., 2010, pp. 51-84. doi: 10.5772/8678 book chapter

[8] Marco, A., Casas, R., Falco, J., Gracia, H., Artigas, J. I., Location-based services for elderly and disabled people. Comput. Commun., 2008, 31, 1055-1066.

[9] Mainetti, L., Patrono, L., A survey on indoor positioning systems. Proc. of 22nd Int. Conf. on Software, Telecommunications and Computer Networks (SoftCOM), Split, Croatia, 7-19 Sept. 2014, pp. 111-120, 2014.

[10] Whitehouse, K., Karlof, C., A practical evaluation of radio signal strength for ranging-based localization. Mob. Comput. Commun. Rev., 2007, 11, 41-52.

[11] Amann, M. C., Bosch, T. M., Lescure, M., Myllylae, R. A., Laser ranging: a critical review of unusual techniques for distance measurement. Opt. Eng., 2001, 40, 10-19.

[12] Yüzbaşioğlu, Ç., Improved range estimation using simple infrared sensors without prior knowledge of surface characteristics. Meas. Sci. Technol., 2005, 16, 1395.

[13] GiPS tech Srl [Online]. Available: http://www.gipstech.com/it/indoor-localization-and-navigation-technology/ [Accessed: 20-Mar-2019].

[14] Ijaz, F., Yang, H. K., Ahmad, A. W., Indoor Positioning: A Review of Indoor Ultrasonic Positioning systems, In the Proceedings of 15th International Conference on Advanced Communications Technology (ICACT), PyeongChang, South Korea, 27-30 January 2013; pp. 1146-1150.

[15] Ureña, J., Hernández, Á., García, J. J., Villadangos, J. M., Acoustic Local Positioning with Encoded Emission Beacons. Proc. IEEE, 2018, 106, 1042-1062,. doi:10.1109/jproc.2018.2819938.

[16] Saad, M. M., Bleakley, C. J., Robust high-accuracy ultrasonic range measurement system. IEEE Trans. Instrum. Meas., 2011, 60, 3334-3341.

[17] Carotenuto, R., Merenda, M., Iero, D., An indoor ultrasonic system for autonomous 3D positioning. IEEE Trans. Instrum. Meas., 2019, 68, 2507-2518,. doi:10.1109/TIM.2018.2866358.

[18] Ho, K. C., Solution and performance analysis of Geolocation by TDOA. IEEE Trans. Aerosp. Electron. Syst. 1993, 29, 1311-1322.

[19] Ruiz, D., Ureña, J., Gude, I., Villadangos, J. M., García, J. C., Pérez, C., New iterative algorithm for hyperbolic positioning used in an Ultrasonic Local Positioning System. In the Proceedings of 2009 IEEE Conference on Emerging Technologies & Factory Automation, Mallorca, Spain, 22-25 September 2009; pp. 1-4. doi:10.1109/etfa.2009.5347237.

[20] Filonenko, V., Cullen, C., Indoor Positioning for Smartphones Using Asynchronous Ultrasound Trilateration. ISPRS Int. J. Geo-Inf., 2013, 2, pp. 598-620. doi:10.3390/ijgi2030598.

[21] Wendeberg, J., Höflinger, F., Schindelhauer, C., Calibration-free TDOA self-localisation. J. Loc. Based Serv., 2013, 7, pp. 121-144. doi: 10.1080/17489725.2013.796410.

[22] Villadangos, J. M., Ureña, J., Mazo, M., Hernández, A., De Marziani, C., Pérez, M. C., Ultrasonic Local Positioning System with Large Covered Area. In the Proceedings of 2007 IEEE International Symposium on Intelligent Signal Processing, Alcala de Henares, Spain, 3-5 October 2007; pp. 1-6. doi:10.1109/wisp.2007.4447508.

[23] Ureña, J., Hernández, A., Jiménez, A., Villadangos, J. M., Mazo, M., García, J. C., Advanced sensorial system for an acoustic LPS. Microprocess. Microsyst., 2007, 31, 393-401.

[24] Saad, M. M., Bleakley, C. J., Ballal, T., High Accuracy Reference-free Ultrasonic Location Estimation. IEEE Trans. Instrum. Meas., 2012, 61, pp. 1561-1570.

[25] Carotenuto R., M. Merenda, D. Iero, and F. G. Della Corte, "Mobile Synchronization Recovery for Ultrasonic Indoor Positioning," Sensors, 2020, 20, 702; doi:10.3390/s20030702.

[26] Choi, H. H., Jin, M. H., Lim, D. W., Lee, S. J., Dilution of Precision Relationship between Time Difference of Arrival and Time of Arrival Techniques with No Receiver Clock Bias User Positioning with Particle Swarm Optimization. J. Electr. Eng. Technol., 2016, 11, pp. 709-718.

[27] Li, X., Deng, Z. D., Rauchenstein, L. T., Contributed Review: Source-localization algorithms and applications using time of arrival and time difference of arrival measurements. Rev. Sci. Instrum., 2016, 87, 041502. doi:10.1063/1.4947001.

[28] Carotenuto R., M. Merenda, D. Iero, and F. G. Della Corte, "Ranging RFID tags with ultrasound," *IEEE Sens. J.*, vol. 18, pp. 2967-2975, 2018. DOI: 10.1109/JSEN.2018.2806564.

[29] Elson, J., Girod, L., Fine-grained time synchronization using reference broadcasts. ACM SIGOPS Operating Syst. Rev., 2002, 36, 147-163.

[30] Carotenuto, R., Merenda, M., Iero, D., Using ANT communications for node synchronization and timing in a wireless ultrasonic ranging system. IEEE Sens. Lett., 2017, 1, 1-4,. doi:10.1109/lsens.2017.2776136

[31] Jackson, J. C., Summan, R., Dobie, G. I., Whiteley, S. M., "Time-of-flight measurement techniques for airborne ultrasonic ranging," IEEE Trans. Ultrason. Ferroelect. Freq. Control, 2013, 60, 343–355.

[32] J. F. Figueroa and E. Barbieri, Position detecting system and method, US Patent 5,280,457, 1992.

[33] J. C. Doyle, B. A. Francis, and A. R. Tannenbaum, "Feedback control theory". Courier Corporation, North Chelmsford, MA, USA, 2013.